

## Flow resistance and velocity distribution in a smooth triangular channel

Hossein Mohammad Nezhad<sup>a</sup>, Mirali Mohammadi <sup>a,\*</sup>, Amir Ghaderi <sup>b</sup>, Mohammad Bagherzadeh<sup>a</sup>, Ana M. Ricardo<sup>c</sup> and Alban Kuriqi<sup>c</sup>

<sup>a</sup> Department of Civil Engineering, Faculty of Engineering, Urmia University, P O Box 165, Urmia 57561-51818, Iran

<sup>b</sup> Department of Civil Engineering, Faculty of Engineering, University of Zanjan, Zanjan 537138791, Iran

<sup>c</sup> CERIS, Instituto Superior Técnico, Universidade de Lisboa, 1049-001, Lisbon, Portugal

\*Corresponding author. E-mail: m.mohammadi@urmia.ac.ir

 MM, 0000-0001-7194-9393; AG, 0000-0002-8661-6302

### ABSTRACT

This study investigates the flow resistance and velocity distribution in a smooth triangular channel under varying slope conditions in a laboratory environment. For this purpose, two triangular cross-sectional shaped channels with 30° and 45° sidewall slopes were made. In various hydraulic conditions, bed slopes were carried out at different flow discharges and channels. The results have been used to test the stage-discharge curve, Manning roughness coefficient,  $n$ , the Darcy-Weisbach friction factor,  $f$ , and flow velocity profiles. By increasing the channel bed slope and flow discharge, the water surface fluctuation increased simultaneously. The fluctuation of flow surface profile in the triangular cross section (TCS) at 45° is more than in TCS 30° cases. The stage-discharge rating curve has less curvature with increasing channel bed slope. The Darcy-Weisbach  $f$  obtained from TCS 30° is higher than for TCS 45°, which means that TCS 30° has more resistance against flowing water passing through the channel than the 45° cross-section. Examination of the velocity contours shows that the maximum velocity occurred in the 30° triangular cross-section. Practical-sound findings from this research might be helpful for hydraulic engineers to design cost-effective open channels and other similar hydraulic structures.

**Key words:** friction factor, manning's roughness, open channel, stage-discharge relationship, velocity contour

### HIGHLIGHTS

- The fluctuation of the water surface profile with triangular cross section (TCS) 30° was higher than for TCS 45°.
- By increasing the slope of the channel, the Darcy-Weisbach ( $f$ ) increases. The  $f$  obtained from TCS 30° is higher than that of TCS 45°.
- With an increase in the channel bed slope, the longitudinal component of velocity increases. Furthermore, the maximum velocity occurred with TCS 30°.

## 1. INTRODUCTION

An accurate prediction of flow resistance in open channels is crucial for sustainable river management and the cost-effective design of hydraulic structures, such as weirs, spillways, and open channels, among others (Saghebian *et al.* 2020; Ghaderi *et al.* 2021). Most approaches for determining flow resistance in open channels use the general concept of boundary shear stress. This concept is based on uniform flow conditions and was initially developed for open channels with gentle slopes (Mohammadi 1998; Aberle & Smart 2003). Open channels under construction commonly lead to sediment deposition on the channel bed, while over-design increases construction cost. Routinely, channel design procedures involve velocity checks at different sections to ensure the adequate conveyance capacity of sediment transport to avoid a deposition (Myers 1982; Javid *et al.* 2018a; Ebtehaj *et al.* 2019). In that regard, shear stress has an essential role in sediment mobility. The distribution of shear stress is uniform in two-dimensional flow. Thus, the shear stress in open channel flows represents the flow resistance, determines the conveyance capacity, and provokes sediment transport (Yen 2002; Mohammadi *et al.* 2015; Ardiçloğlu & Kuriqi 2019; Mohammadi & Moludi 2021). In general, the most popular semi-empirical flow resistance models such as Chézy, Manning, and Darcy–Weisbach show a nonlinear relationship between energy losses and mean flow velocity (Banerjee *et al.* 2019; Daneshfaraz *et al.* 2021).

This is an Open Access article distributed under the terms of the Creative Commons Attribution Licence (CC BY 4.0), which permits copying, adaptation and redistribution, provided the original work is properly cited (<http://creativecommons.org/licenses/by/4.0/>).

Nevertheless, the validation of those models is made through experimental and/or field data investigations. Consequently, the literature has already proposed a wide range of calibration coefficients. Therefore, no unique calibration coefficient covers different geometries and hydraulic components in open channels. However, the flow in open channels of finite aspect ratio is three-dimensional. Wall shear stress is not distributed uniformly on wetted perimeters due to free surface and secondary current and changes in channel slope (Myers 1982; Glaister 1993, 1995; Javid *et al.* 2018b). The computation of the friction coefficient,  $f$ , is a challenging task due to the complexity of the problem in an open channel flow with a finite aspect ratio.

Furthermore, while conventional approaches can provide adequate accuracy in predicting  $f$  in pipe flow, it is widely accepted that the accuracy of the conventional methods is insufficient in open channel flow (Mohammadi 2001; Bilgil & Altun 2008). As  $f$  is a fundamental parameter in the computation of flow discharge, practical and accurate techniques are still highly demanded. Thus, the accurate estimation of flow resistance and its variability are essential for stable channel design, mitigating high discharges hazards, fluvial ecosystem rehabilitation, and river morphodynamics prediction (Righetti & Armanini 2002; Sun & Shiono 2009). Different factors influence flow resistance; nevertheless, it is widely recognized that the most important ones are: the channel shape, dimensions, the arrangement of elements that form the roughness, cross-sectional shape, vegetation, and dissipative effects triggered by macro-vortices due to flow separation in abrupt changes of direction (Cowan 1956). The skin resistance, resistance induced by the boundary surface that depends upon the flow depth relative to the size of roughness elements on the boundary surface, is one of the main components of flow resistance. At the same time, another critical component of flow resistance is form drag associated with the bed features that influence secondary circulations and eddies (Mohammadi 2008; Mazumder & Sarkar 2014). Therefore, the overall Manning's coefficient,  $n$ , can be expressed as the sum of the relevant values. Although accurate estimation of flow resistance in open channels is of great interest to hydraulic engineers, the problem remains unsolved despite numerous studies done over the past decades. The main challenge arises in assessing the sidewall effect on flow resistance. In practice, the bed and geomorphology of the open channels are continually changing due to interaction with the flow (Yang & Tan 2008). While there is a handful of studies that investigate the influence of bed slope on hydraulic properties (Dey & Debnath 2000; Aberle & Smart 2003; Banerjee *et al.* 2019), to the best of our knowledge, the influence of the sidewall geometry and slope on hydraulic regimes remains scarcely investigated. Therefore, the main objective of this study is to investigate the hydraulic properties such as flow resistance and velocity distribution in a smooth triangular channel under varying slope conditions considering different discharge releases in a laboratory environment. Thus, this study's novelty and main contribution stand in providing some new insights on how sidewall geometry and slope influence the full hydraulic performance of a channel that is crucial in practice for constructing cost-effective irrigation and/or drainage channels. The rest of the paper is organized as follows: Section 2 briefly describes the experimental work conducted in the hydraulics laboratory at Urmia University (Iran) and its limitations. Section 3 presents the main results and discussions of the relevance of the key findings achieved in this study. Finally, the main conclusions drawn from this study are presented in Section 4.

## 2. EXPERIMENTAL APPARATUS AND PROCEDURES

### 2.1. Experimental setup

The laboratory tests were performed in a rectangular tilting flume of 0.3 m width, 0.5 m depth, and 15 m length at the Hydraulics Laboratory of Urmia University. The sidewalls were made of transparent glass to improve flow visibility and reduce friction. The slope of the channel is adjustable with a hydraulic jack (Ghaderi *et al.* 2020). The schematic design of the experimental setup is shown in Figure 1.

A recirculation pump with a maximum discharge rate of 24 L/s was used to supply water to the head tank from the storage tanks. An ultrasonic flowmeter with a precision of  $\pm 1$  L/s was used on the transmission pipe to measure the flow discharge. A honeycomb planar mesh was added to reduce turbulence in the entrance region. In addition, a tailgate was installed at the end of the channel to control the inflow conditions with the intended flow depth (Ghaderi & Abbasi 2021). Two triangular-shaped channels with 30° and 45° sidewall slopes were made of glass with five different channel bed slopes. After stabilizing the flow conditions, the flow depth was determined for both the upstream and downstream sections by a pointer gauge mounted on the top of the flume with an accuracy of  $\pm 1$  mm. Table 1 shows the geometric parameters and the main hydraulic properties of the experimental rig.

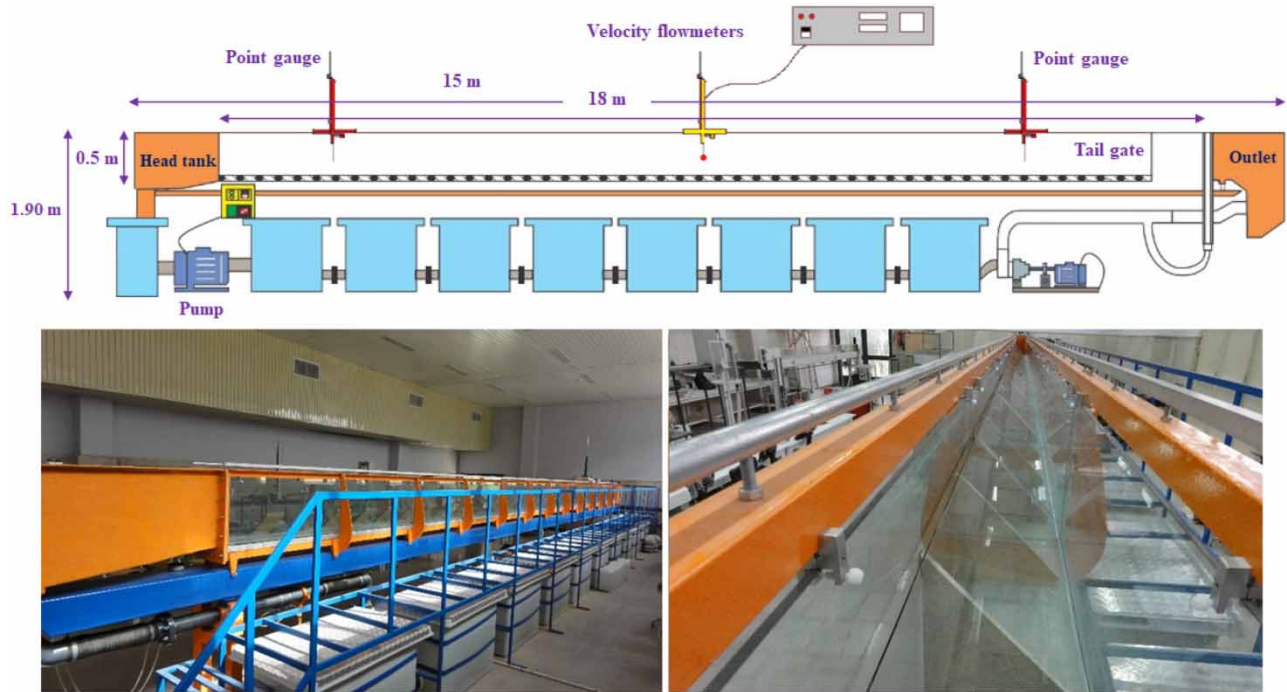


**Figure 1** | Schematic view and photographs of the experimental setup.

**Table 1** | Geometric parameters and flow characteristics of the experimental channel

Parameter	Dimension	Range
Discharge	L/s	5.65–20.55
Velocity	m/s	0.45–1.67
Flow depth	m	0.093–0.387
Sidewall slope	–	30° and 45°
Bed slope, S	–	0.001–0.016
Froude number, Fr	–	0.6–2.95

The flow velocity was measured using a propeller velocity flowmeter H32-1A (produced by Armfield Engineering Co.: <https://armfield.co.uk>) positioned over the channel centerline. This flowmeter is used to measure very low point velocities in water. It uses the impedance of a rotating multi-bladed propeller to indicate rotational speed caused by the flowing fluid. The flow velocity varied between 25 and 3,000 mm/s with an accuracy of  $\pm 1$  mm/s (see Figure 2).

## 2.2. Limitations of experiments

Open channels are important water transfer structures used in water resources systems. As such, they may require a substantial amount of investment depending on their length and cross-section. Therefore, cross-section design should be carried out on an optimization basis. A channel section is defined as the cross-section perpendicular to the main flow direction. A triangular channel is an open channel with a triangular cross-section. One side is vertical, and the other is inclined. In practice, it is known that secondary currents might be present for straight open channels. The patterns of secondary currents are affected by the aspect ratio of the channel, the roughness of the bottom and walls, and the shape of the cross-section (Tominaga *et al.* 1989; Blanckaert *et al.* 2010). Blanckaert *et al.* (2010) confirm these implications and elaborate on the influence of roughness on trapezoidal channels. The demonstrated influence of the cross-sectional shape in a straight channel already indicates that this parameter might be influential in a confluence as well. In particular, depending on the cross-



**Figure 2** | Propeller velocity flowmeter (Armfield 3000 mm/s – H32-1A model).

sectional shape, the incoming channels of the confluence will have a different fully developed velocity profile, which might result in different mixing of these two streams. Additionally, the shape of the confluence area itself might influence the extent of flow features like the contraction and the separation zone. However, for the sake of the simplification of the experimental design, those issues were overlooked, and it was assumed that there were no confluence or secondary channels connected to the channel.

### 3. RESULTS AND DISCUSSION

#### 3.1. Free surface profile and flow discharge estimation

Figure 3 shows the water surface profile for different discharges having different channel bed slopes ( $S$ ), i.e., 0.001, 0.002, 0.004, 0.008, and 0.016. As can be seen from the figure, when the channel bed slope gets steeper, the flow depth decreases. The decrease is sharp for the outlet of the channel bed slope compared to the channel's inlet. The water surface fluctuations increased by increasing the channel bed slope and flow discharge. The results show that the fluctuation of water surface profile in triangular cross section (TCS)  $30^\circ$  was higher than in TCS  $45^\circ$ . Also, the decrease of water depth in the channel outlet was more abrupt in TCS  $30^\circ$  than in TCS  $45^\circ$ .

Regression analysis of the data from different channel bed slopes and two-channel cross-sections was conducted to find the stage-discharge rating curve. Mathematically, the stage-discharge relationship is expressed by Equation (1) as:

$$Q = a(y)^b \quad (1)$$

where  $Q$  is the flow discharge (L/s),  $y$  is the stage (m), and  $a$  and  $b$  are adjustment parameters. From Figure 4, it was observed that in the case of a steeper channel bed slope (i.e.,  $S = 0.016$ ), the increase in the stage is comparatively less than for the gentle channel bed slope (i.e.,  $S = 0.004$ ) for the same flow discharges.

In other words, by increasing channel bed slope, the stage-discharge rating curve has less curvature, which can be attributed the higher increase in flow velocity in a steep channel than to its lower increase in the gentle channel. Some parameter values from  $a$  and  $b$  are proposed in Table 2 to estimate the stage-discharge relationship for different values in the channel bed slopes and cross-section of the channel.

The coefficient of determination ( $R^2$ ) of the stage-discharge relationships indicated a good fit with different values of channel bed slope. From Table 2, it can be seen that by increasing the slope of the channel, the value  $a$  decreases for both cross-sectional cases. For TCS  $30^\circ$ , by increasing the channel bed slope,  $b$  remains almost the same, whereas, for TCS  $45^\circ$ , by increasing the slope of the channel,  $b$  increases, which means that the stage-discharge rating curve has increasingly less curvature.

#### 3.2. Flow resistance coefficient

The roughness coefficients represent the resistance of friction that water experiences when it flows over land or a channel characterized by specific geomorphological characteristics. Flow resistance is traditionally represented in one of two ways. The commonest is a fixed value of  $n$  in the Manning equation:

$$V = \frac{1}{n} R^{2/3} S^{1/2} \quad (2)$$

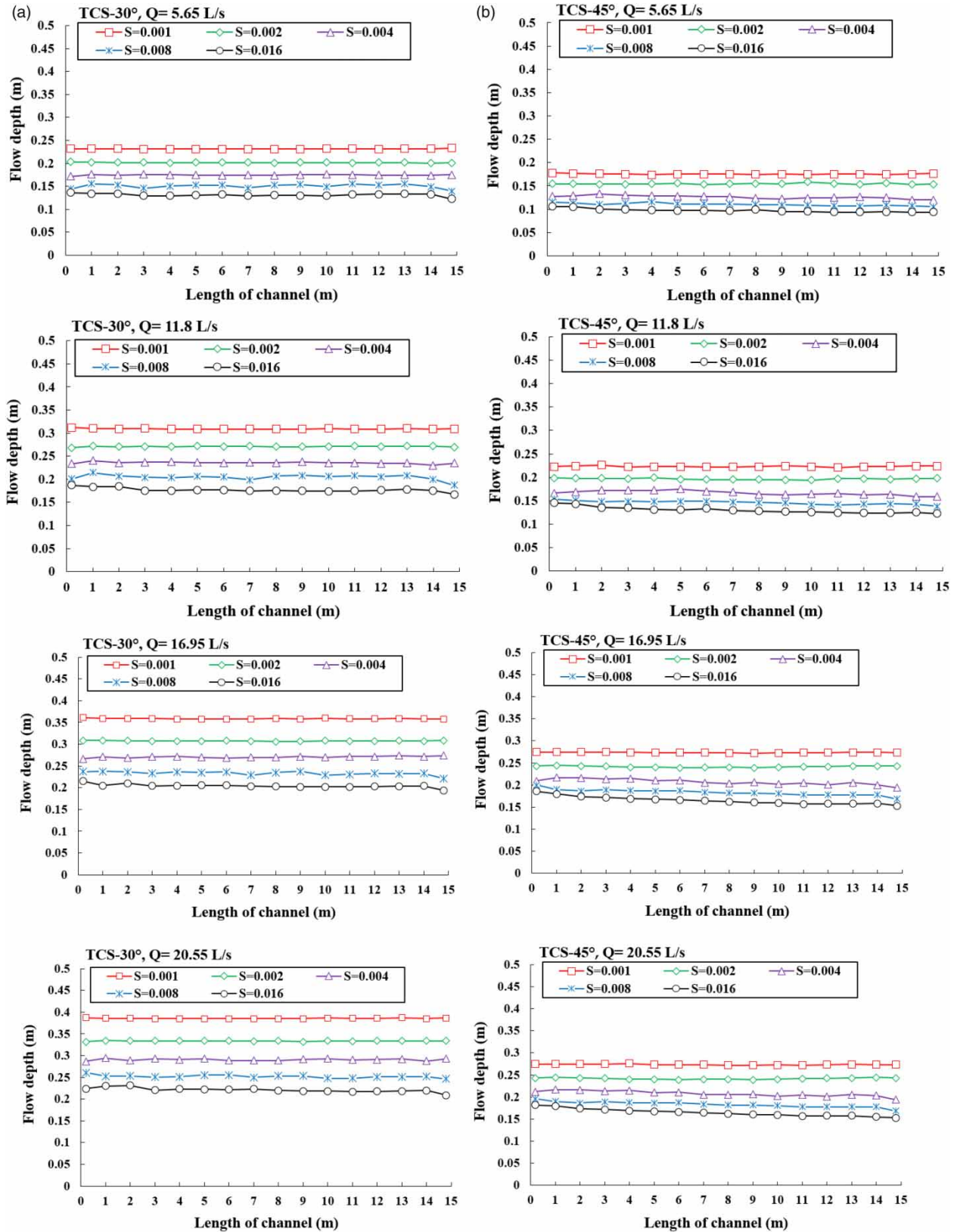


**Figure 3** | Water surface profile for triangular cross-sections for different bed and sidewall channel slopes: (a) TCS-30° and (b) TCS-45°.

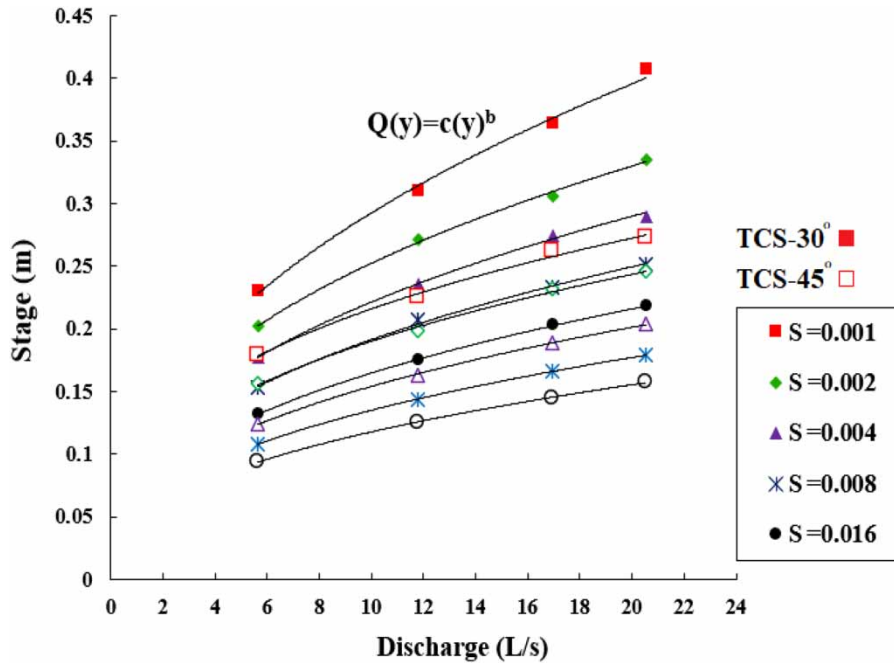


**Figure 4** | Stage-discharge rating curves for two cross-sections of the channel.

**Table 2** | Proposed values of coefficients  $a$  and  $b$  in Equation (1) for various channel bed slopes

Cross section	Channel bed slope (S)	$a$	$b$	$R^2$
30°	0.001	107.54	0.435	0.996
	0.002	103.58	0.386	0.998
	0.004	90.43	0.388	0.998
	0.008	79.38	0.382	0.997
	0.016	67.12	0.389	0.999
45°	0.001	99.93	0.334	0.995
	0.002	83.59	0.357	0.996
	0.004	63.43	0.385	0.999
	0.008	54.84	0.391	0.998
	0.016	46.88	0.4	0.998

where  $V$  is mean velocity,  $R$  is hydraulic radius and  $S$  denotes the channel bed slope. And the other two main alternative parameters are provided by the fixed value of the Darcy-Weisbach friction factor ( $f$ ) and the acceleration due to gravity ( $g$ ):

$$V = (8gRS/f)^{1/2} \quad (3)$$

Figure 5 further presents the variation of Manning's  $n$  with flow discharge along the different bed slopes of the channel. Over the full range of flow discharge, the values of  $n$  are reduced with TCS 45° compared to TCS 30°.

A decrease has occurred because the cross-sectional sidewall's slope increases from 30° to 45°. In other words, a triangular channel with a 30° cross-section has more resistance against flowing water passing through the channel than a 45° cross-section. As shown in Figure 5, the values of  $n$  increase by increasing discharge for each cross-section. By increasing  $n$  values, the flow depth in the channel decreases. For steep slopes where the flow regime is supercritical, the values of  $n$  are close to each other. However, for the gentle slopes where the flow regime is subcritical, the values of  $n$  are pretty different to each other (Cowan 1956). It was noticed that the average  $n$  values were found between 0.008 and 0.0075 for steep

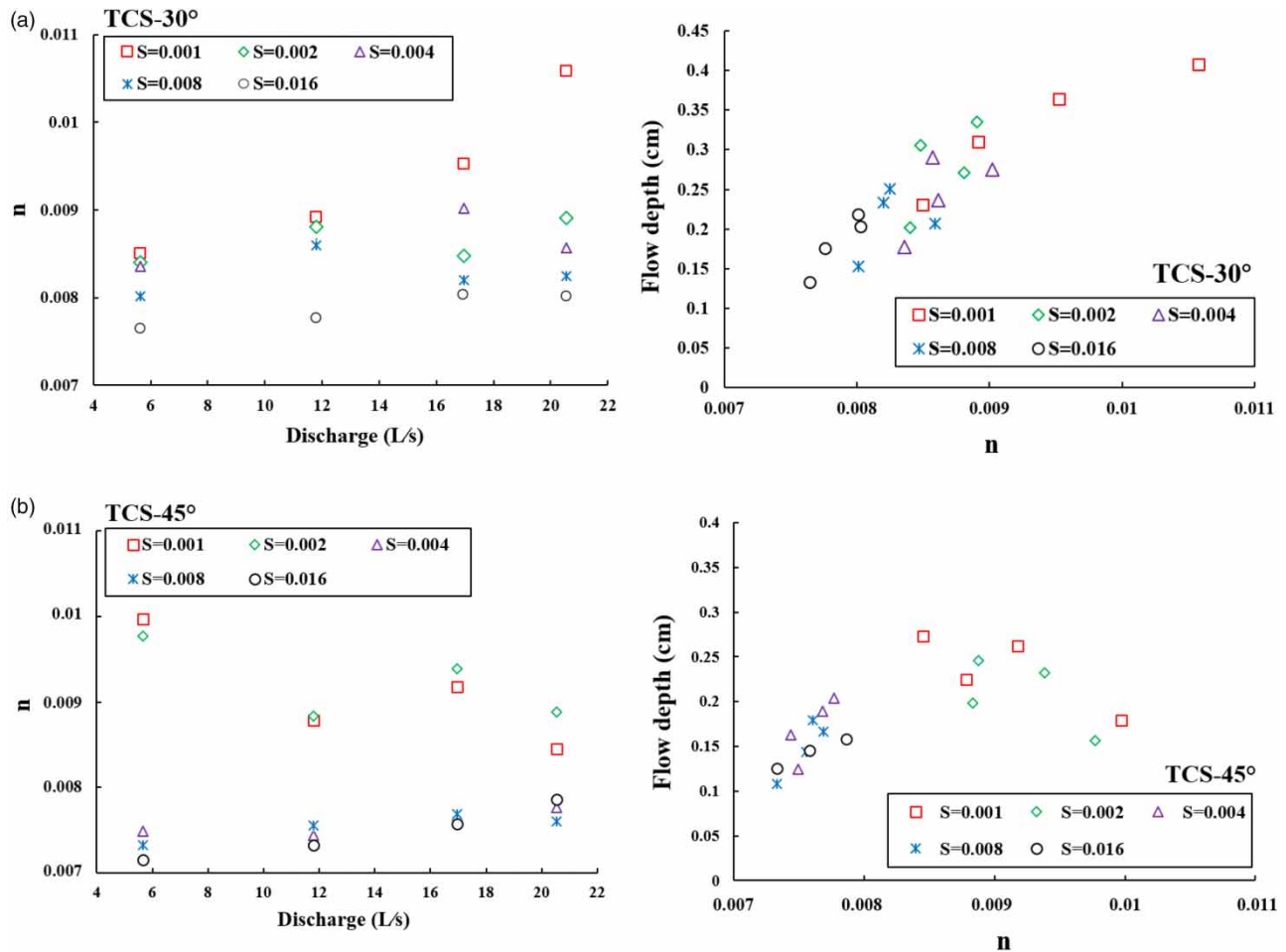


**Figure 5** | Variation of Manning's  $n$  versus flow discharge and flow depth. (a) TCS-30° and (b) TCS-45°.

slopes and 0.0095 and 0.0085 for gentle slopes in the case of 30° and 45°, respectively. The variation of Darcy-Weisbach friction factor,  $f$ , with discharge along the different slopes of the channel is illustrated in Figure 6. It is inferred from Figure 6 that the trend of Darcy-Weisbach  $f$  for both cross-sections of the channel is the same, and the values of  $f$  decrease by increasing flow discharge or water flow depth (Myers 1982; Yen 2002).

Here, it is noted that by increasing the channel's bed slope ( $S$ ), the Darcy-Weisbach  $f$  increases (Bilgil & Altun 2008). Also, for the same discharge values, the Darcy-Weisbach  $f$  obtained from TCS 30° is higher than at TCS 45°. This means that in the same flow conditions, resistance against flowing water passing through the channel in the TCS 45° case is less than in TCS 30°.

### 3.3. Velocity distribution

Figure 7 presents the 2D velocity distribution for cross-sections, namely TCS 45° and 30° with a different channel bed slope. It appears that the velocity closest to the wall is almost zero in all models.

However, a higher velocity occurs in the central part of the triangle cross-section, slightly above the center of gravity of a triangle and near the free surface. By comparing the velocity contours between two cross-sections, it can be seen that the maximum velocity occurred in a 30° triangular cross-section; with an increase in the slope of the channel, the longitudinal component of velocity increases (Banerjee *et al.* 2019).

Figure 8 shows the maximum velocity for different flow discharge values within the two cross-sections of the channel. There is almost the same trend between the maximum velocity and discharge passing through two different cross-sections of triangular channels. However, as seen from this figure, the calculated  $V_{max}$  at TSC 45° is higher than at TSC 30° for the

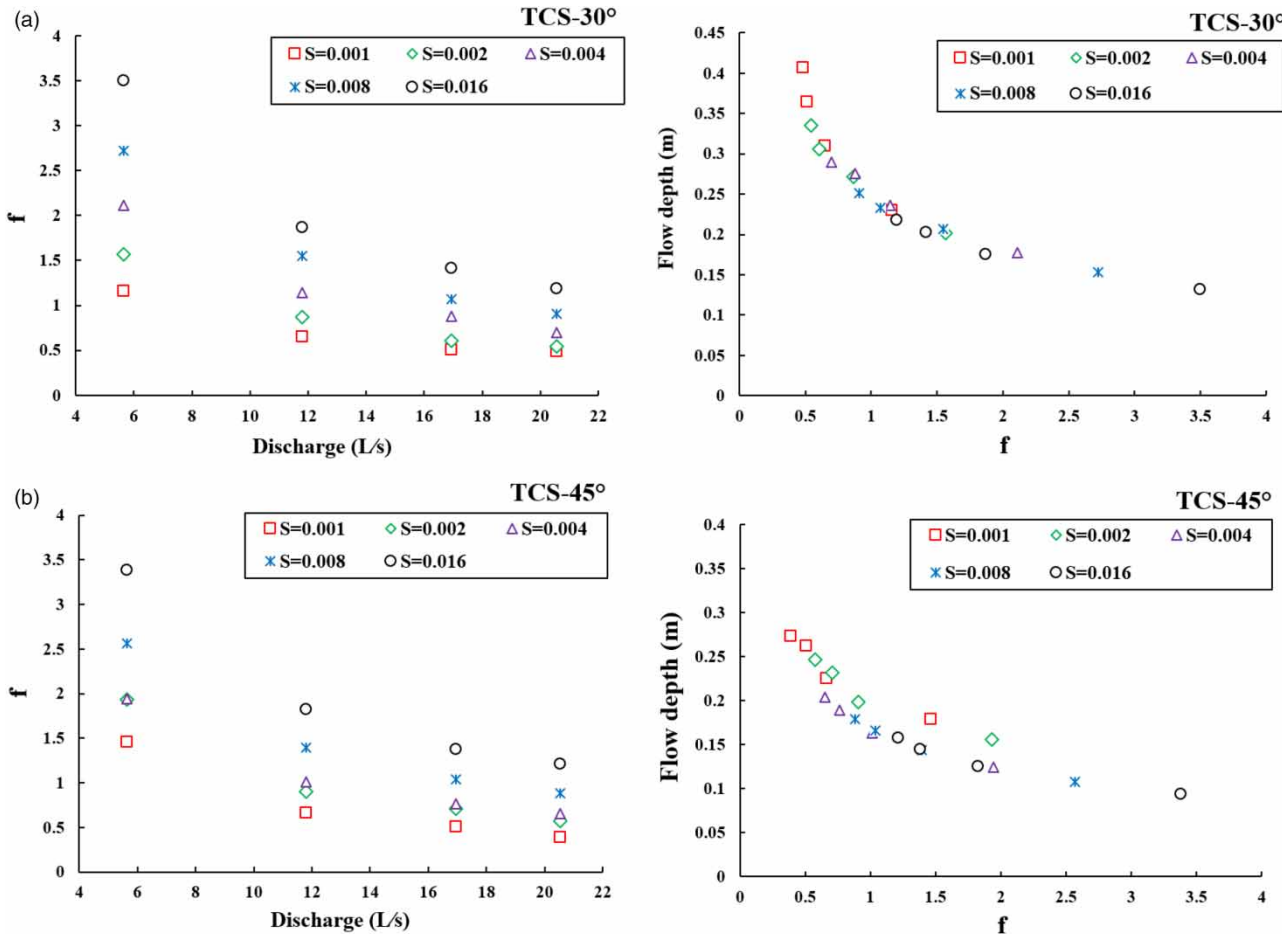


**Figure 6** | Variation of Darcy-Weisbach  $f$  versus flow discharge and flow depth. (a) TCS-30° and (b) TCS-45°.

same conditions. This difference may be attributed to common resistance against flowing water passing through the channel in TCS 30° and TCS 45° cases (Myers 1982; Yang & Tan 2008).

#### 4. CONCLUSIONS

The experimental work studied flow resistance and velocity distributions in two triangular-shaped channels considering five different channel bed slopes. In addition, experiments were carried out for the stage-discharge relationship, Manning's  $n$ , the Darcy-Weisbach  $f$ , and flow velocity profiles in various hydraulics conditions. The following major conclusions are drawn.

The water surface fluctuations increased by increasing the channel bed slope and flow discharge. The fluctuation of the water surface profile in TCS 30° was higher than in TCS 45°. This is because the stage-discharge rating curve has less curvature.

The values of  $n$  increase by increasing flow discharge for each cross-section. By increasing  $n$  values, the flow depth of the channel decreases. However, the average  $n$  values were found between 0.008 and 0.0075 for steep slopes and 0.0095 and 0.0085 for gentle slopes in the cases of 30° and 45°, respectively.

By increasing the slope of the channel, the Darcy-Weisbach  $f$  increases. At TSC 30°, the flow resistance is higher than at TSC 45°. This means that resistance against flowing water passing through the channel in the case of TCS 45° is less than in TCS 30° case, in the same flow conditions. In addition, the values of  $f$  are more sensitive than the  $n$  values.

The higher velocity occurs in the central part of the triangle cross-section and near the free surface; the longitudinal velocity component increases with an increase in the channel bed slope. Furthermore, the maximum velocity occurred in a 30° triangular cross-section.



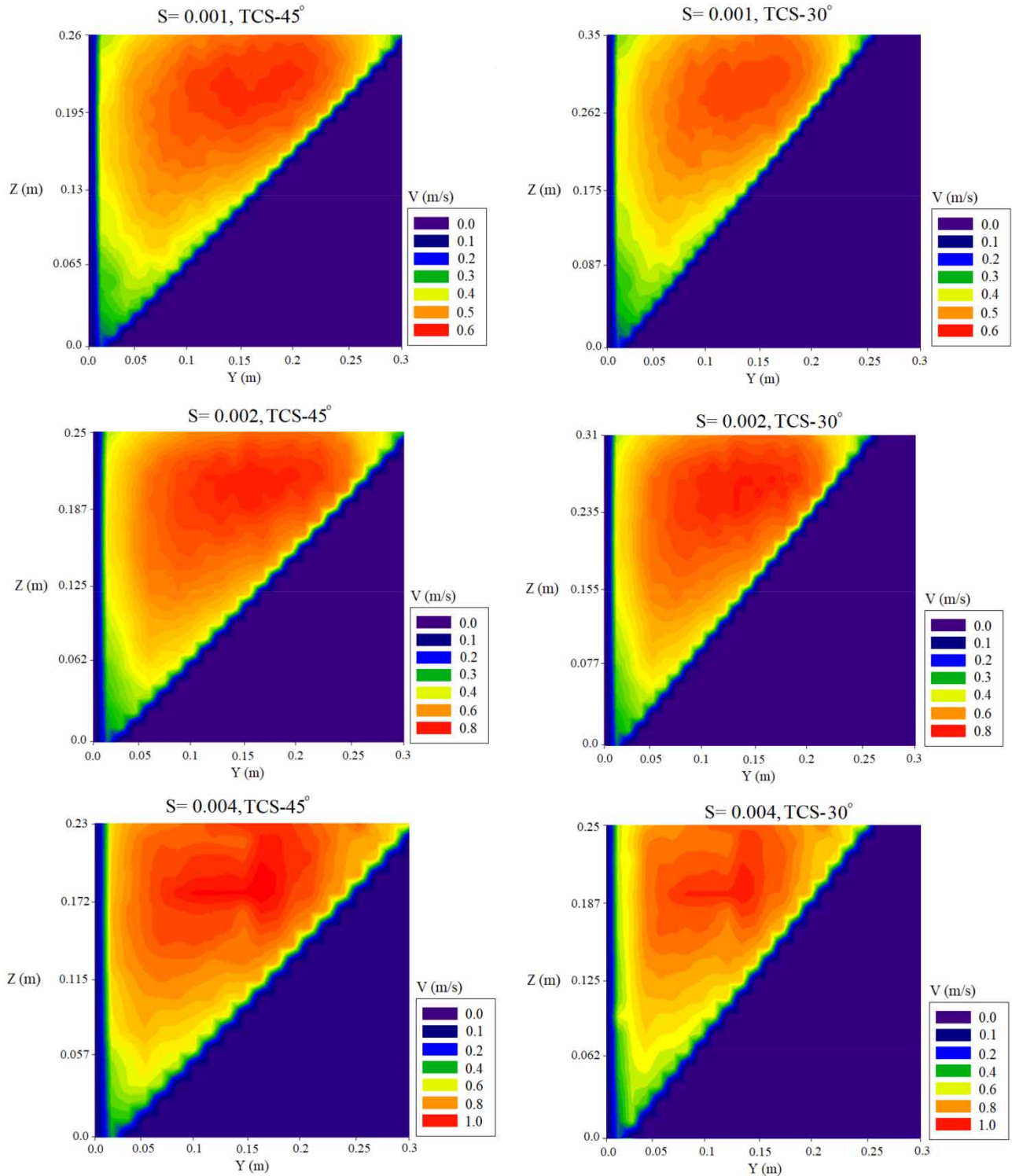


**Figure 7** | Velocity distribution in a triangular channel with different sloped walls and bed slopes. (continued).

Although the values of  $n$  have been practiced and investigated in hydraulics and hydrology analysis, the determination of  $n$  is becoming a challenge to engineers and researchers because its value cannot be computed equally for all types of open channels. The velocity distribution in hydraulic structures is essential to understand most fluid flow problems, flow resistances, and

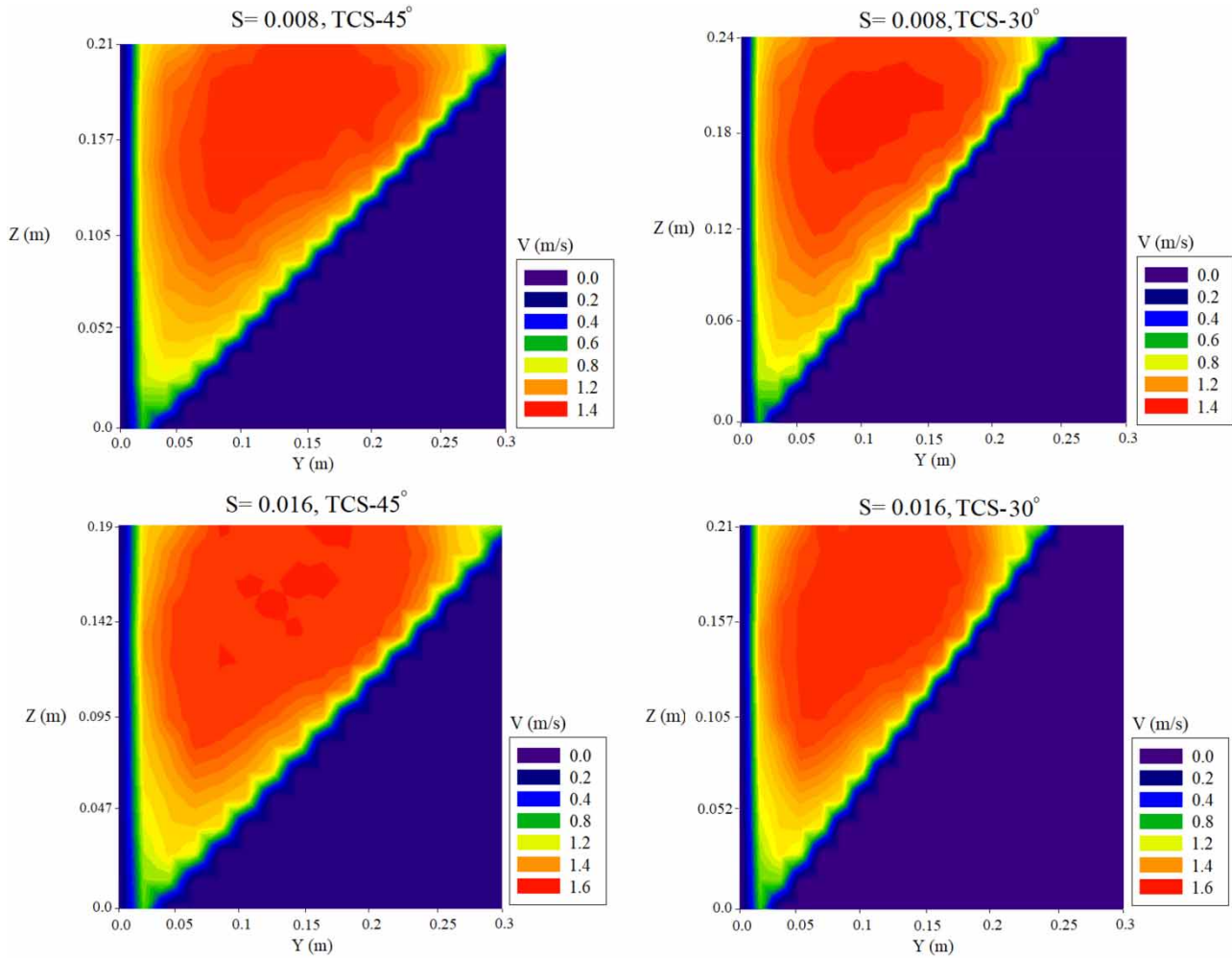


Figure 7 | Continued.

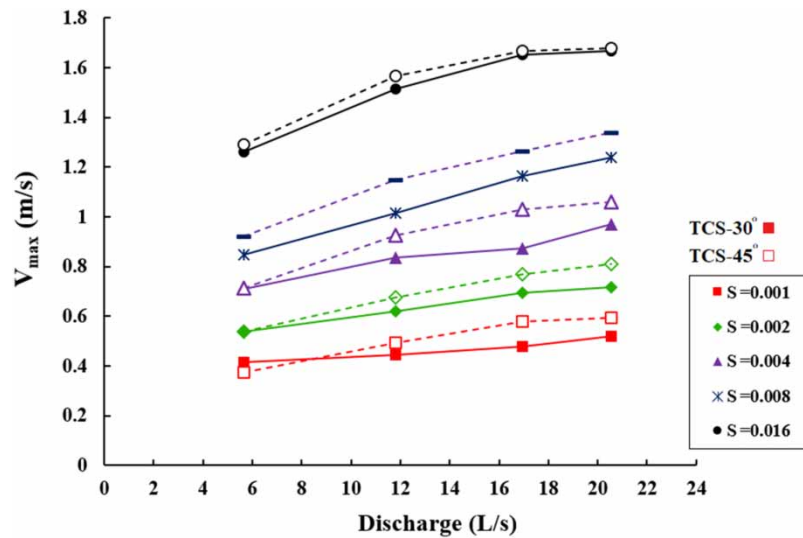


Figure 8 | Maximum velocity values in triangular channels with different channel bed slopes.

sediment transport. Due to the lack of data and laboratory studies, a research laboratory in this field can significantly help understand several aspects and features of hydraulic regimes in open channels. In this regard, for many practical applications, the determination of  $n$  in natural channels with the river crossing during the flood is needed. Therefore, future work remains an issue to be faced.

## DATA AVAILABILITY STATEMENT

All relevant data are included in the paper or its Supplementary Information.

## REFERENCES

- Aberle, J. & Smart, G. M. 2003 The influence of roughness structure on flow resistance on steep slopes. *Journal of Hydraulic Research* **41** (3), 259–269.
- Ardıçlıoğlu, M. & Kuriqi, A. 2019 Calibration of channel roughness in intermittent rivers using HEC-RAS model: case of Sarımsaklı creek, Turkey. *SN Applied Sciences* **1** (9), 1080.
- Banerjee, S., Naik, B., Singh, P. & Khatua, K. K. 2019 Flow resistance in gravel bed open channel flows case: intense transport condition. *ISH Journal of Hydraulic Engineering* **25** (3), 298–309.
- Bilgil, A. & Altun, H. 2008 Investigation of flow resistance in smooth open channels using artificial neural networks. *Flow Measurement and Instrumentation* **19** (6), 404–408.
- Blanckaert, K., Duarte, A. & Schleiss, A. J. 2010 Influence of shallowness, bank inclination and bank roughness on the variability of flow patterns and boundary shear stress due to secondary currents in straight open-channels. *Advances in Water Resources* **33** (9), 1062–1074.
- Cowan, W. L. 1956 Estimating hydraulic roughness coefficients. *Agricultural Engineering* **37** (7), 473–475.
- Daneshfaraz, R., Aminvash, E., Ghaderi, A., Abraham, J. & Bagherzadeh, M. 2021 SVM performance for predicting the effect of horizontal screen diameters on the hydraulic parameters of a vertical drop. *Applied Sciences* **11** (9), 4238.
- Dey, S. & Debnath, K. 2000 Influence of streamwise bed slope on sediment threshold under stream flow. *Journal of Irrigation Drainage Engineering* **126** (4), 255–263.
- Ebtehaj, I., Bonakdari, H. & Es-haghi, M. S. 2019 Design of a hybrid ANFIS–PSO model to estimate sediment transport in open channels. *Iranian Journal of Science and Technology, Transactions of Civil Engineering* **43** (4), 851–857.
- Ghaderi, A. & Abbasi, S. 2021 Experimental and numerical study of the effects of geometric appendage elements on energy dissipation over stepped spillway. *Water* **13** (7), 957.
- Ghaderi, A., Abbasi, S. & Di Francesco, S. 2021 Numerical study on the hydraulic properties of flow over different pooled stepped spillways. *Water* **13** (5), 710.
- Ghaderi, A., Daneshfaraz, R., Torabi, M., Abraham, J. & Azamathulla, H. M. 2020 Experimental investigation on effective scouring parameters downstream from stepped spillways. *Water Supply* **20** (5), 1988–1998.
- Glaister, P. 1993 A numerical scheme for two-dimensional, open channel flows with non-rectangular geometries. *International Journal of Engineering Science* **31** (7), 1003–1011.
- Glaister, P. 1995 Prediction of steady, supercritical, free-surface flow. *International Journal of Engineering Science* **33** (6), 845–854.
- Javid, S., Mohammadi, M., Najarchi, M. & Najafi Zadeh, M. 2018a Laboratory investigation of flow resistance in composite roughened rectangular open channels. *Journal of Fresenius Environmental Bulletin* **27** (7), 4921–4929.
- Javid, S., Mohammadi, M., Najarchi, M. & Najafi Zadeh, M. 2018b An experimental study of the effect of boundary roughness in rectangular open channels. *Water and Soil Science* **28** (4), 95–107.
- Mazumder, B. S. & Sarkar, K. 2014 Turbulent flow characteristics and drag over 2-D forward-facing dune shaped structures with two different stoss-side slopes. *Environmental Fluid Mechanics* **14** (3), 617–645.
- Mohammadi, M. 1998 *Resistance to Flow and the Influence of Boundary Shear Stress on Sediment Transport in Smooth Rigid Boundary Channels*. PhD Thesis, University of Birmingham.
- Mohammadi, M. 2001 Shape effects and definition of hydraulic radius in Manning's equation in open channel flow. *International Journal of Engineering* **10** (3), 127–142.
- Mohammadi, M. 2008 Local and global friction factor in a channel with v-shaped bottom. *International Journal of Engineering* **21** (4), 325–336.
- Mohammadi, M. & Moludi, M. 2021 Determination of Resistance Coefficient in Gravel Bed Rivers (Case Study: Urmia Shahr-Chay River). *Water and Soil Science*. In Press. DOI: 10.22034/WS.2021.12251.
- Mohammadi, M. A., Mohammad Nejad, H. & Ebrahim Nejadian, H. 2015 Flow resistance and velocity distributions in channels with triangular cross-section. *Experimental Research in Civil Engineering* **2** (3), 55–66.
- Myers, W. 1982 Flow resistance in wide rectangular channels. *Journal of the Hydraulics Division* **108** (4), 471–482.
- Righetti, M. & Armanini, A. 2002 Flow resistance in open channel flows with sparsely distributed bushes. *Journal of Hydrology* **269** (1), 55–64.
- Saghebani, S. M., Roushangar, K., Ozgur Kirca, V. S. & Ghasempour, R. 2020 Modeling total resistance and form resistance of movable bed channels via experimental data and a kernel-based approach. *Journal of Hydroinformatics* **22** (3), 528–540.

- Sun, X. & Shiono, K. 2009 Flow resistance of one-line emergent vegetation along the floodplain edge of a compound open channel. *Advances in Water Resources* **32** (3), 430–438.
- Tominaga, A., Nezu, I., Ezaki, K. & Nakagawa, H. 1989 Three-dimensional turbulent structure in straight open channel flows. *Journal of Hydraulic Research* **27** (1), 149–173.
- Yang, S.-Q. & Tan, S.-K. 2008 Flow resistance over mobile bed in an open-channel flow. *Journal of Hydraulic Engineering* **134** (7), 937–947.
- Yen, B. C. 2002 Open channel flow resistance. *Journal of Hydraulic Engineering* **128** (1), 20–39.

First received 13 December 2021; accepted in revised form 10 March 2022. Available online 22 March 2022